Anomalous Dressing of Dirac Fermions in the Topological Surface State of Bi_2Se_3, Bi_2Te_3, and Cu-Doped Bi_2Se_3

Takeshi Kondo,* Y. Nakashima, Y. Ota, Y. Ishida, W. Malaeb, K. Okazaki, and S. Shin†
ISSP, University of Tokyo, Kashiwa, Chiba 277-8581, Japan

M. Kriener, Satoshi Sasaki, Kouji Segawa, and Yoichi Ando‡
Institute of Scientific and Industrial Research, Osaka University, Osaka 567-0047, Japan
(Received 29 December 2012; published 23 May 2013)

Quasiparticle dynamics on the topological surface state of Bi_2Se_3, Bi_2Te_3, and superconducting $Cu_xBi_2Se_3$ are studied by 7 eV laser-based angle resolved photoemission spectroscopy. We find strong mode couplings in the Dirac-cone surface states at energies of ~3 and ~15–20 meV associated with an exceptionally large coupling constant λ of ~3, which is one of the strongest ever reported for any material. This result is compatible with the recent observation of a strong Kohn anomaly in the surface phonon dispersion of Bi_2Se_3, but it appears that the theoretically proposed "spin-plasmon" excitations realized in helical metals are also playing an important role. Intriguingly, the ~3 meV mode coupling is found to be enhanced in the superconducting state of $Cu_xBi_2Se_3$.

DOI: 10.1103/PhysRevLett.110.217601 PACS numbers: 79.60.−i, 71.38.Cn, 72.15.Nj, 73.20.−r

Topological insulators (TIs) are a new class of materials with Dirac fermions appearing on the surface [1]. The nature of Dirac fermions has already been actively studied in the graphitic materials [2], and it has been elucidated that the Dirac band dispersion is anomalously renormalized by such effects as electron-phonon interaction, electron-hole pair generation, and electron-plasmon coupling, leading to various intriguing properties [3–5]. While topological insulators are essentially understood within the noninteracting topological theory [6–8], the Dirac fermions realized in actual materials would be affected by nontrivial many body interactions, and hence the investigation of the quasiparticle dynamics is important for extending our understanding beyond the noninteracting regime. Since the Dirac fermions in TIs are distinct from those in graphitic materials in terms of their helical spin texture as well as possible interactions with a separate bulk electronic state, the low-energy excitations in the topological surface state are of particular interest. Indeed, such excitations are important not only for understanding many body interactions in the topological surface sate, but also for assessing the stability of putative Majorana fermions that are expected to emerge on the surface of superconducting TIs [9,10].

In this context, there are already indications of the significance of many body interactions in the topological surface state. For example, a pronounced Kohn anomaly to indicate a strong electron-phonon coupling was recently observed in the surface phonon branch of Bi_2Se_3 [11]; scanning tunneling spectroscopy (STS) uncovered an intriguing feature with finely resolved sharp peaks at low energies (<20 meV) in the Landau-level spectra [12], pointing to an anomalous increase in the quasiparticle lifetime near the Fermi energy (E_F). Theoretically, it has been proposed that a novel low-energy collective mode called "spin plasmon" emerges as a consequence of the spin-momentum locking in the topological surface state [13]. Therefore, it is important to elucidate how the Dirac dispersion is renormalized close to E_F. However, so far the angle-resolved photoemission spectroscopy (ARPES) has not been able to detect any significant renormalization in the Dirac dispersions in TIs [14], possibly because of the lack of sufficient energy resolutions.

In this Letter, we demonstrate that the Dirac dispersion of the topological surface state is indeed anomalously renormalized, by using state-of-the-art ARPES with a 7-eV laser photon source. The availability of ultrahigh energy resolution (~1 meV) and extremely low temperature (~1 K) [15] enabled us to detect low-energy kinks in the dispersion at ~3 and ~15–20 meV, giving evidence for hitherto-undetected mode couplings. The analysis of the kinks leads to the estimate of the coupling constant λ of as large as ~3, which is one of the largest reported for any material [16,17]. Nevertheless, we observed no overall band reconstruction down to the lowest temperature, indicating that the topological surface state are protected from density-wave formations, which is usually expected to occur with such an extremely strong coupling with bosons [18–22].

Single crystals of Bi_2Se_3 and Bi_2Te_3 were grown by melting stoichiometric amounts of elemental shots in sealed evacuated quartz glass tubes. Superconducting samples of $Cu_{0.24}Bi_2Se_3$ with T_c of 3.5 K and a shielding fraction of ~30% [see Fig. 3(a)] were prepared by electrochemically intercalating Cu into the pristine Bi_2Se_3 [23–26]. ARPES measurements were performed using a Scienta R4000 hemispherical analyzer with an ultraviolet laser ($h\nu = 6.994$ eV) at the Institute for Solid State Physics (ISSP), University of Tokyo [27,28].

Figures 1(a1)–(a5) and (b1)–(b5) show the ARPES data of Bi_2Se_3 and Bi_2Te_3, respectively. The Dirac cones are clearly seen in the dispersion maps [see Figs. 1(a2) and (b2)], and the Fermi surface (FS) shapes are very different between the two compounds [see Figs. 1(a3) and (b3)]. In this experiment, we did not observe any quantum-well states which emerge when adsorption of residual gases on the surface causes charge doping [29–34]. Also, our data are free from spectral intensity from the bulk conduction band, as can be clearly seen in Figs. 1(a1) and (b1) where the momentum distribution curves (MDCs) at E_F show only two sharp peaks from the surface state. This situation prevents complex scattering channels that could affect the spectral line shape and complicates the interpretation of renormalization effects [35,36].

The novel feature in our data is that the MDC-derived band dispersions [see Figs. 1(a4) and (b4)] obviously deviate from straight lines, pointing to a large mass enhancement; the renormalized slope of the dispersion close to E_F is shown by dashed lines. As shown in the upper insets of Figs. 1(a4) and (b4), we calculate the energy difference between the putative linear dispersion and the measured one to estimate the strength of the coupling as a function of energy. We found anomalies at two energies, ~ -15 and ~ -3 meV, indicative of electron couplings with two different kinds of collective modes.

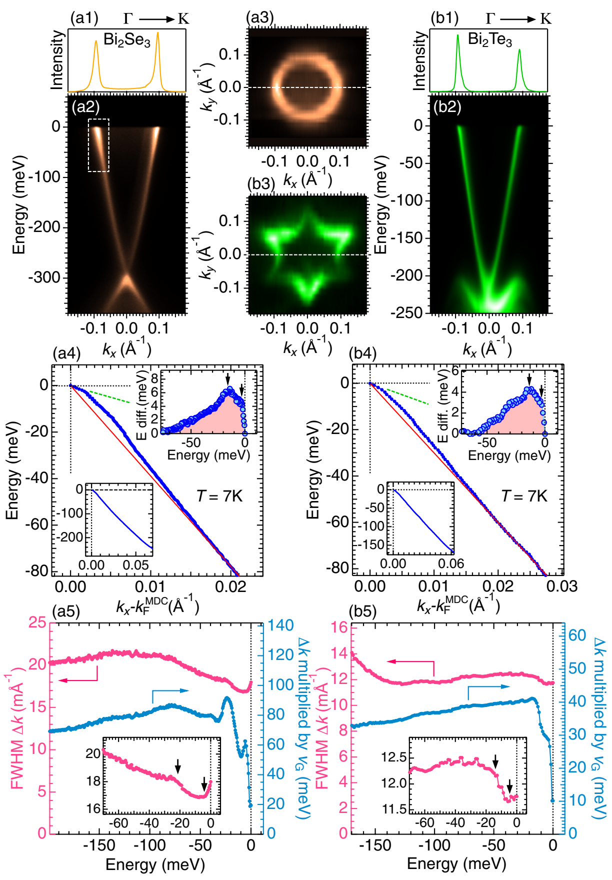

FIG. 1 (color online). Data for (a1)–(a5) Bi_2Se_3 and (b1)–(b5) Bi_2Te_3. (a1),(b1) MDC at E_F. (a2),(b2) Band dispersion map along Γ–K [dashed lines in (a3) and (b3)]. (a3),(b3) Fermi surface map. (a4),(b4) MDC-derived band dispersions near E_F obtained from the data shown in panels (a2) and (b2). The same dispersion over a wide energy range is shown in the lower-left inset. The upper-right inset plots the energy difference from the linear dispersion. (a5),(b5) MDC peak width Δk [full width at half maximum (FWHM)], and the $\Delta k(E)$ multiplied by the group velocity $v_G(E)$. The inset shows the $\Delta k(E)$ close to E_F.

The effects of the couplings should also be observed in the energy dependence of the MDC peak width (Δk). In Figs. 1(a5) and (b5), we plot the obtained spectrum of Δk for Bi_2Se_3 and Bi_2Te_3, respectively; as expected, $\Delta k(E)$ presents kinks at the two energy scales, $\sim -(15–20)$ and ~ -3 meV, which are better seen in the insets. The ~ -3 meV kink marks the onset of an anomalous increase in the magnitude of $\Delta k(E)$ toward E_F, which is unusual; we have confirmed the reproducibility of this low-energy feature in many samples and concluded that it is an intrinsic property of the topological surface state.

To understand the complex behavior of the band dispersions revealed at low energy, we examine the shapes of the energy distribution curves (EDCs) around k_F shown in Fig. 2(c). In Fig. 2(d), those original EDCs are divided by the Fermi function at the measured temperature of 7 K convoluted with the experimental energy resolution to remove the effect of the Fermi cutoff. In the resulting curves, one can identify up to three shoulderlike features [an example for $k_x - k_F^{\mathrm{EDC}} = 0.018$ Å^{-1} is shown in Fig. 2(b)], and the energy positions of those features are plotted on the ARPES image shown in Fig. 2(a). One can see in Fig. 2(d) that one of the shoulderlike features on the curves actually corresponds to the maximum; the dispersion of this maximum close to k_F is also plotted in Fig. 2(a) with thick filled symbols, and this dispersion is fitted with a parabolic dashed line in Fig. 2(a), giving a significantly enhanced effective mass of $0.83m_e$ (m_e is the free-electron mass). For comparison, we also plot a putative band dispersion with a mass of $0.14m_e$, which was estimated for the bulk band from quantum oscillations [37]. The mass enhancement realized in the topological state is remarkable. Even more surprisingly, the estimated value of $\lambda = v_0/v_F - 1$ (v_0 and v_F are the bare-electron velocity [38] and the renormalized Fermi velocity, respectively) is as large as ~ 3 as demonstrated in Fig. 2(a), which is one of the strongest couplings ever reported in any material [16,17]. This value is also much larger than that previously reported ($\lambda < 0.3$) for Bi_2Se_3 based on less straightforward estimates [14,39].

Perhaps the most direct way to demonstrate the strong mode coupling is to present the peak-dip-hump structure in the EDCs. In Fig. 2(e), we show EDCs at k_F and beyond, where the peak-dip-hump shape is usually emphasized, and indeed, a clear dip can be seen at ~ -16 meV

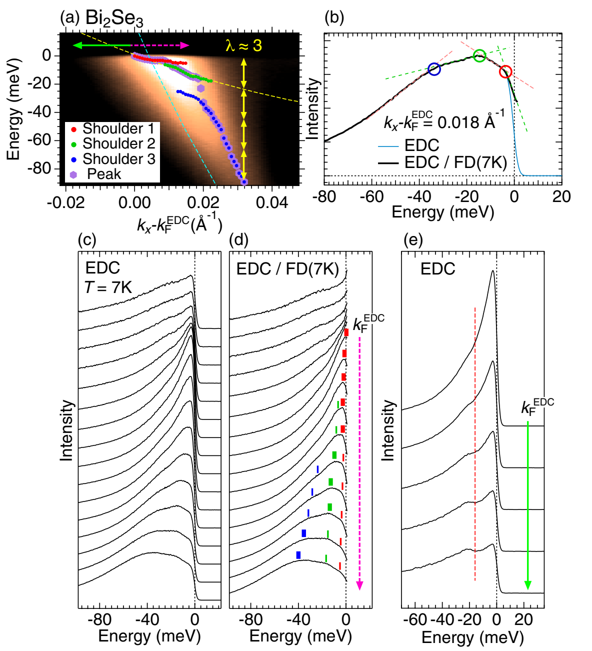

FIG. 2 (color online). Data for Bi_2Se_3 within a narrow range near E_F marked in Fig. 1(a2). (a) ARPES image; parabolic bands (dashed lines) with a mass of $0.83m_e$ and $0.14m_e$ [37] are superimposed. (b) Typical EDC with three features. (c) EDCs near k_F on the occupied-state side, and (d) those divided by the Fermi function at $T = 7$ K. Energies of shoulderlike structures [circles in (b) and bars in (d)] are plotted on (a). The energy eigenvalue for each k, $\varepsilon(k)$, which is determined by the energy positions at which the spectral intensity becomes maximum, are indicated in (d) with bold bars, and plotted in (a) with thick filled hexagons. (e) EDCs beyond k_F (unoccupied-state side). The dashed line indicates the energy of the spectral dip.

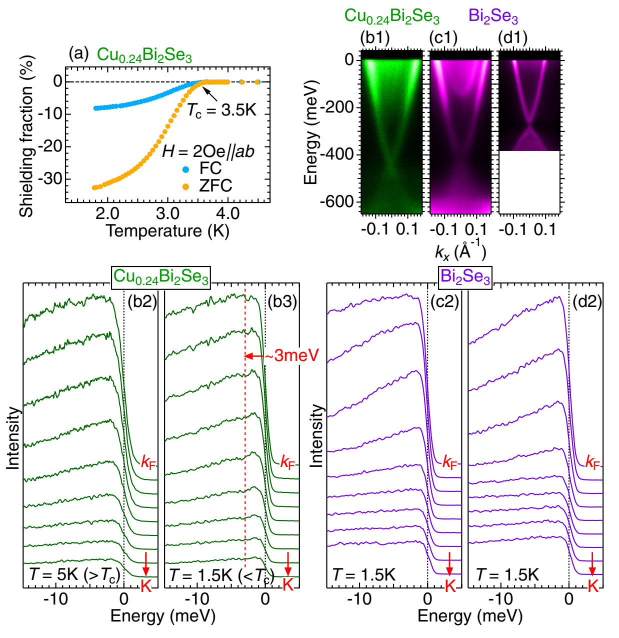

FIG. 3 (color online). Data for $Cu_{0.24}Bi_2Se_3$ superconductor with $T_c = 3.5$ K and the pristine Bi_2Se_3. (a) Field-cooled (FC) and zero-field-cooled (ZFC) data of the superconducting shielding fraction of the sample used for ARPES experiments. Band dispersion map along Γ-K for (b1) $Cu_{0.24}Bi_2Se_3$, (c1) aged, and (d1) fresh surfaces of Bi_2Se_3. EDCs of $Cu_{0.24}Bi_2Se_3$ close to k_F measured (b2) above T_c and (b3) below T_c. The dashed line in (b3) indicates the spectral dip. EDCs of the pristine Bi_2Se_3 close to k_F for (c2) aged and (d2) fresh surfaces.

(dashed line). On the other hand, the ~3 meV mode does not give rise to such a peak-dip-hump feature in Bi_2Se_3, manifesting itself only as a weak kink in EDCs.

Intriguingly, we found that a peak-dip-hump structure becomes visible at ~3 meV in superconducting samples of Cu-doped Bi_2Se_3. Figures 3(b2) and (b3) show the EDCs of $Cu_{0.24}Bi_2Se_3$ with $T_c = 3.5$ K measured above and below T_c, respectively. The peak-dip-hump structure is seen at ~3 meV below T_c but it is gone above T_c. We also measured the pristine Bi_2Se_3 at the same condition ($T = 1.5$ K), but did not observe the peak-dip-hump [see Fig. 3(d2)]. Furthermore, we doped the surface of the pristine sample up to a doping level similar to that of $Cu_{0.24}Bi_2Se_3$ by exposing it to residual gases [compare Figs. 3(c1) and (d1)], but again, the peak-dip-hump structure is not observed [see Fig. 3(c2)]. Obviously, the enhancement of the ~3 meV mode coupling has something to do with the superconductivity, and the origin of this enhancement needs to be scrutinized in future studies. In passing, we note that we did not detect any signature of the superconducting energy gap in the present experiment, probably because the superconductivity is inhomogeneous in this material [26]. More elaborate studies would be required to nail down the topological superconductivity in $Cu_xBi_2Se_3$ [25] by ARPES experiments.

Now we show the relevance of the mode couplings to the scattering rate ($1/\tau$), which we try to extract from our data in two ways: one simply uses the peak width of the EDCs ($\Delta\varepsilon = 1/\tau$), the raw data of which are shown in Figs. 4(b) and 4(c); the other calculates the product of the MDC width and the renormalized group velocity $v_G(E)$ ($\Delta k v_G \approx 1/\tau$), where $v_G(E)$ is obtained by differentiating the $\varepsilon(k)$ data shown in Figs. 1(a4) and (b4). The $1/\tau$ scattering rate is not exactly the same as the imaginary part of the self-energy, because it now includes the effect of the real part. However, multiplying Δk by v_G would cancel the effect of the spectral-weight shift due to mode couplings, which can cause the unusual upturn of Δk toward E_F seen in Figs. 1(a5) and (b5), and it makes the proper energy dependence of the scattering rate become visible. Indeed, the E dependence of $\Delta k v_G$ is consistent with that of $\Delta\varepsilon$ (which is a straightforward measure of the scattering rate of quasiparticles), as shown in Fig. 4(a) for Bi_2Te_3. Reassuringly, the behavior of $\Delta k v_G$ in both Bi_2Se_3 and Bi_2Te_3 clearly reflects the mode couplings at ~20 and ~3 meV [see Figs. 1(a5) and (b5)], corroborating the existence of two modes.

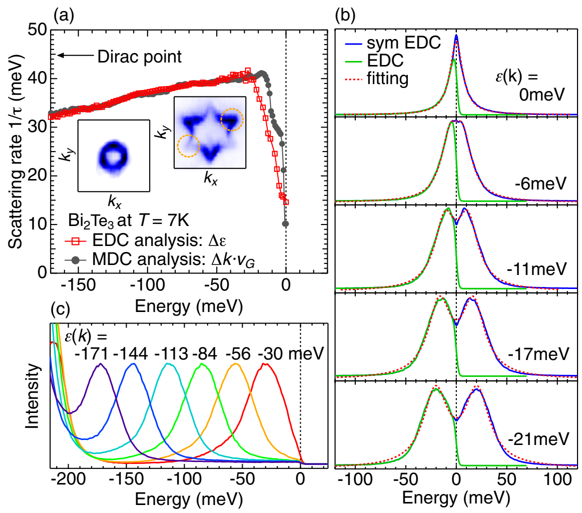

FIG. 4 (color online). Results for Bi_2Te_3. (a) Scattering rate ($1/\tau$) estimated from EDC peak width $\Delta\varepsilon$ (FWHM) as well as from the MDC peak width multiplied by the group velocity $\Delta k v_G$. Insets show the ARPES map at -150 meV (left) and E_F (right). (b) Estimation of $\Delta\varepsilon$ by fitting double Lorentzians to the symmetrized EDCs. (c) EDCs far from k_F; the energy eigenvalue for each k, $\varepsilon(k)$, corresponds to the peak position in each EDC.

One may notice in Fig. 4(a) that both $\Delta\varepsilon$ and $\Delta k v_G$ reduce sharply toward E_F. This behavior appears to be consistent with the STS result showing a sharpening of Landau-level peaks at low energies (<20 meV) [12]. Another notable feature in $1/\tau$ is that it gradually decreases toward the Dirac point. This is unusual, because a monotonic increase in the electron-electron interaction with increasing binding energy is usually expected in conventional metals [40]. We speculate that this unusual behavior is a consequence of the fact that the penetration depth of the surface state increases as the momentum moves away from the Dirac point [41], which makes the surface state gradually gain some bulk character. In fact, a feature to suggest such a variation is seen in the energy-contour maps plotted in the inset of Fig. 4(a): the contour near the Dirac point (left image) is almost circular, but close to E_F (right image), it exhibits a C_3 modulation reflecting the symmetry of the bulk.

Now we discuss the most crucial question, namely, the origin of the bosons causing the anomalies at $\sim -(15$–$20)$ and ~ -3 meV in the ARPES spectra. A plausible candidate for the higher binding-energy one is the out-of-plane optical phonon mode A_{1g}^2 with $\omega = 21$ and 16 meV for Bi_2Se_3 and Bi_2Te_3, respectively [42,43]. It seems that Δk begins to decrease toward E_F [see Figs. 1(a5) and (b5)] at almost the same energy as that of the A_{1g}^2 mode. Also, the relevance of the phonon coupling is supported by the fact that the mode energy observed in Bi_2Se_3 (~ 20 meV) is higher than that in Bi_2Te_3 (~ 15 meV), which is consistent with the mass difference between Se and Te ($\sqrt{m_{Te}/m_{Se}} = 1.27$).

As for the ~ 3 meV mode, there are two possible origins. One is the optical mode of surface phonons. Recently, a strong Kohn anomaly was detected by a helium atom surface scattering (HASS) experiment in a phonon branch of Bi_2Se_3 [11] at approximately $2k_F^{Dirac}$ (k_F^{Dirac} is the Fermi momentum on the Dirac cone) with the characteristic energy of ~ 3 meV, and this Kohn anomaly was attributed to the surface optical phonon mode [11]. While this Kohn anomaly [44] may actually play some role in the strong renormalization observed in our ARPES data, the λ value obtained in the HASS experiment for the relevant phonons was only 0.43 [47], which is too small to account for the very strong coupling observed here for the ~ 3 meV mode. Therefore, the surface optical phonons alone are obviously not sufficient for understanding the lower energy mode, and we need to seek additional ingredients.

In this respect, another, more promising, origin of the ~ 3 meV mode is the theoretically proposed spin plasmon, which is suggested to have a maximum energy of ~ 2.2 meV [13]. This mode consists of coupled plasmons and spin waves, and unlike the Kohn anomaly [21], it is expected for the round FS as in Bi_2Se_3 [13]. Indeed, in our ARPES data the ~ 3 meV mode coupling is obviously stronger in Bi_2Se_3 than in Bi_2Te_3 where the FS is warped. The unusual upturn observed in the MDC width toward E_F [see the insets of Figs. 1(a5) and (b5)] could be interpreted to signify increasingly stronger interactions of the Dirac fermions with spin plasmons near E_F. Note that such strong interactions between the two are expected only when the plasmon spectrum does not overlap with the continuum of electron-hole excitations [3,48], and hence the plasmon coupling should dominate the scatterings with $q \sim 0$. Therefore, it is natural that the quasiparticle scattering is enhanced toward E_F in this spin-plasmon scenario. All told, it is most likely that the large-angle scattering ($q \sim 2k_F$) by the surface optical phonons and the small-angle scattering ($q \ll 2k_F$) by the spin plasmons are both playing roles in the enormously strong mass enhancement observed near E_F on the topological surface state.

In conclusion, we have investigated the quasiparticle dynamics in the topological surface state of Bi_2Se_3, Bi_2Te_3, and $Cu_xBi_2Se_3$. We found strong mode couplings at binding energies of ~ 15–20 and ~ 3 meV. The coupling to the A_{1g}^2 phonons is proposed as the candidate for the former mode. As for the ~ 3 meV mode, there are two possible origins. One is the optical mode of surface phonons. The other is the spin plasmons, which are theoretically proposed as low-energy excitations of the helically spin-polarized Dirac fermions. Intriguingly, despite the extremely large mass enhancement factor λ of ~ 3, the topological surface state remains free from any band reconstruction down to the lowest temperature, indicating that the helical Dirac cone is protected from density-wave formations which are naturally expected for a system with extremely strong couplings to bosons.

This work is supported by JSPS (FIRST Program, NEXT Program, KAKENHI 23740256 and KAKENHI 24740218), MEXT (Innovative Area "Topological Quantum Phenomena" KAKENHI 22103004), and AFOSR (AOARD 124038).

*kondo1215@issp.u-tokyo.ac.jp
†shin@issp.u-tokyo.ac.jp
‡y_ando@sanken.osaka-u.ac.jp

[1] M.Z. Hasan and C.L. Kane, Rev. Mod. Phys. **82**, 3045 (2010).
[2] A.H. Castro Neto, N.M.R. Peres, K.S. Novoselov, and A.K. Geim, Rev. Mod. Phys. **81**, 109 (2009).
[3] A. Bostwick, T. Ohta, T. Seyller, K. Horn, and E. Rotenberg, Nat. Phys. **3**, 36 (2007).
[4] Y. Zhang, V.W. Brar, F. Wang, C. Girit, Y. Yayon, M. Panlasigui, A. Zettl, and M.F. Crommie, Nat. Phys. **4**, 627 (2008).
[5] Y. Liu, L. Zhang, M.K. Brinkley, G. Bian, T. Miller, and T.-C. Chiang, Phys. Rev. Lett. **105**, 136804 (2010).
[6] L. Fu, C.L. Kane, and E.J. Mele, Phys. Rev. Lett. **98**, 106803 (2007).
[7] J.E. Moore and L. Balents, Phys. Rev. B **75**, 121306(R) (2007).
[8] X.-L. Qi, T.L. Hughes, and S.-C. Zhang, Phys. Rev. B **78**, 195424 (2008).
[9] L. Fu and C.L. Kane, Phys. Rev. Lett. **100**, 096407 (2008).
[10] P. Hosur, P. Ghaemi, R.S.K. Mong, and A. Vishwanath, Phys. Rev. Lett. **107**, 097001 (2011).
[11] X. Zhu, L. Santos, R. Sankar, S. Chikara, C. Howard, F.C. Chou, C. Chamon, and M. El-Batanouny, Phys. Rev. Lett. **107**, 186102 (2011).
[12] T. Hanaguri, K. Igarashi, M. Kawamura, H. Takagi, and T. Sasagawa, Phys. Rev. B **82**, 081305(R) (2010).
[13] S. Raghu, S.B. Chung, X.-L. Qi, and S.-C. Zhang, Phys. Rev. Lett. **104**, 116401 (2010).
[14] Z.-H. Pan, A.V. Fedorov, D. Gardner, Y.S. Lee, S. Chu, and T. Valla, Phys. Rev. Lett. **108**, 187001 (2012).
[15] K. Okazaki *et al.*, Science **337**, 1314 (2012).
[16] W.L. McMillan, Phys. Rev. **167**, 331 (1968).
[17] P. Hofmann, I.Y. Sklyadneva, E.D.L. Rienks, and E.V. Chulkov, New J. Phys. **11**, 125005 (2009).
[18] K. Nasu, Phys. Rev. B **44**, 7625 (1991).
[19] C.R. Ast and H. Höchst, Phys. Rev. Lett. **90**, 016403 (2003).
[20] Y.M. Koroteev, G. Bihlmayer, J. Gayone, E. Chulkov, S. Blügel, P. Echenique, and Ph. Hofmann, Phys. Rev. Lett. **93**, 046403 (2004).
[21] E.W. Plummer, J. Shi, S.-J. Tang, E. Rotenberg, and S.D. Kevan, Prog. Surf. Sci. **74**, 251 (2003).
[22] L. Fu, Phys. Rev. Lett. **103**, 266801 (2009).
[23] M. Kriener, K. Segawa, Z. Ren, S. Sasaki, S. Wada, S. Kuwabata, and Y. Ando, Phys. Rev. B **84**, 054513 (2011).
[24] M. Kriener, K. Segawa, Z. Ren, S. Sasaki, and Y. Ando, Phys. Rev. Lett. **106**, 127004 (2011).
[25] S. Sasaki, M. Kriener, K. Segawa, K. Yada, Y. Tanaka, M. Sato, and Y. Ando, Phys. Rev. Lett. **107**, 217001 (2011).
[26] M. Kriener, K. Segawa, S. Sasaki, and Y. Ando, Phys. Rev. B **86**, 180505(R) (2012).
[27] T. Kiss *et al.*, Phys. Rev. Lett. **94**, 057001 (2005).
[28] T. Kiss, T. Shimojima, K. Ishizaka, A. Chainani, T. Togashi, T. Kanai, X.-Y. Wang, C.-T. Chen, S. Watanabe, and S. Shin, Rev. Sci. Instrum. **79**, 023106 (2008).
[29] P.D.C. King *et al.*, Phys. Rev. Lett. **107**, 096802 (2011).
[30] M. Bianchi, R.C. Hatch, J. Mi, B.B. Iversen, and P. Hofmann, Phys. Rev. Lett. **107**, 086802 (2011).
[31] Z.-H. Zhu *et al.*, Phys. Rev. Lett. **107**, 186405 (2011).
[32] H.M. Benia, C. Lin, K. Kern, and C.R. Ast, Phys. Rev. Lett. **107**, 177602 (2011).
[33] L.A. Wray, S.-Y. Xu, Y. Xia, D. Hsieh, A.V. Fedorov, Y.S. Hor, R.J. Cava, A. Bansil, H. Lin, and M.Z. Hasan, Nat. Phys. **7**, 32 (2011).
[34] M. Bianchi, D. Guan, S. Bao, J. Mi, B.B. Iversen, P.D.C. King, and P. Hofmann, Nat. Commun. **1**, 128 (2010).
[35] S.R. Park, W.S. Jung, C. Kim, D.J. Song, C. Kim, S. Kimura, K.D. Lee, and N. Hur, Phys. Rev. B **81**, 041405(R) (2010).
[36] S.R. Park *et al.*, New J. Phys. **13**, 013008 (2011).
[37] K. Eto, Z. Ren, A.A. Taskin, K. Segawa, and Y. Ando, Phys. Rev. B **81**, 195309 (2010).
[38] v_0 was estimated from the slope of the putative linear dispersion in the absence of mode couplings, shown as solid straight lines in Figs. 1(a4) and (b4).
[39] R.C. Hatch, M. Bianchi, D. Guan, S. Bao, J. Mi, B.B. Iversen, L. Nilsson, L. Hornekær, and P. Hofmann, Phys. Rev. B **83**, 241303(R) (2011).
[40] T. Valla, A.V. Fedorov, P.D. Johnson, and S.L. Hulbert, Phys. Rev. Lett. **83**, 2085 (1999).
[41] W. Zhang, R. Yu, H.-J. Zhang, X. Dai, and Z. Fang, New J. Phys. **12**, 065013 (2010).
[42] W. Richter, H. Kohler, and C.R. Becker, Phys. Status Solidi B **84**, 619 (1977).
[43] K.M.F. Shahil, M.Z. Hossain, D. Teweldebrhan, and A.A. Balandin, Appl. Phys. Lett. **96**, 153103 (2010).
[44] It is useful to note that the Kohn anomaly is typically accompanied by an extensive FS nesting and is very anisotropic [21,45,46]; however, in Bi_2Se_3 no nesting is present [see Fig. 1(a3)] and the HASS experiment found the anomaly to be isotropic [11]. Hence, the Kohn anomaly in Bi_2Se_3 is obviously unusual.
[45] E. Hulpke and J. Lüdecke, Phys. Rev. Lett. **68**, 2846 (1992).
[46] E. Rotenberg, J. Schaefer, and S.D. Kevan, Phys. Rev. Lett. **84**, 2925 (2000).
[47] X. Zhu, L. Santos, C. Howard, R. Sankar, F.C. Chou, C. Chamon, and M. El-Batanouny, Phys. Rev. Lett. **108**, 185501 (2012).
[48] P. Hawrylak, Phys. Rev. Lett. **59**, 485 (1987).